Title

SHOC2-MRAS-PP1 complex positively regulates RAF activity and contributes to Noonan syndrome pathogenesis.

Journal

Proceedings of the National Academy of Sciences of the United States of America, 115(45)

ISSN

0027-8424

Authors

Young, Lucy C
Hartig, Nicole
Boned Del Río, Isabel
et al.

Publication Date

2018-11-01

DOI

10.1073/pnas.1720352115

Peer reviewed

SHOC2–MRAS–PP1 complex positively regulates RAF activity and contributes to Noonan syndrome pathogenesis

Lucy C. Young[a,1], Nicole Hartig[a,2], Isabel Boned del Río[a], Sibel Sari[a], Benjamin Ringham-Terry[a], Joshua R. Wainwright[a], Greg G. Jones[a], Frank McCormick[b,3], and Pablo Rodriguez-Viciana[a,3]

[a]University College London Cancer Institute, University College London, London WC1E 6DD, United Kingdom; and [b]Helen Diller Family Comprehensive Cancer Center, University of California, San Francisco, CA 94158

Contributed by Frank McCormick, September 18, 2018 (sent for review November 22, 2017; reviewed by Deborah K. Morrison and Marc Therrien)

Dephosphorylation of the inhibitory "S259" site on RAF kinases (S259 on CRAF, S365 on BRAF) plays a key role in RAF activation. The MRAS GTPase, a close relative of RAS oncoproteins, interacts with SHOC2 and protein phosphatase 1 (PP1) to form a heterotrimeric holoenzyme that dephosphorylates this S259 RAF site. MRAS and SHOC2 function as PP1 regulatory subunits providing the complex with striking specificity against RAF. MRAS also functions as a targeting subunit as membrane localization is required for efficient RAF dephosphorylation and ERK pathway regulation in cells. SHOC2's predicted structure shows remarkable similarities to the A subunit of PP2A, suggesting a case of convergent structural evolution with the PP2A heterotrimer. We have identified multiple regions in SHOC2 involved in complex formation as well as residues in MRAS switch I and the interswitch region that help account for MRAS's unique effector specificity for SHOC2–PP1. MRAS, SHOC2, and PPP1CB are mutated in Noonan syndrome, and we show that syndromic mutations invariably promote complex formation with each other, but not necessarily with other interactors. Thus, Noonan syndrome in individuals with SHOC2, MRAS, or PPPC1B mutations is likely driven at the biochemical level by enhanced ternary complex formation and highlights the crucial role of this phosphatase holoenzyme in RAF S259 dephosphorylation, ERK pathway dynamics, and normal human development.

RAS | SHOC2 | MRAS | PP1 | Noonan syndrome

Up-regulation of the RAS–RAF–MEK–ERK signaling pathway is one of the most common drivers of human cancer and is also responsible for a family of developmental disorders known as RASopathies (1, 2). Within this signaling cascade, regulation of RAF kinases in particular is an intricate process involving multiple phosphorylation/dephosphorylation events and interactions with regulatory proteins (3). RAF is maintained in an autoinhibited "closed" conformation in the cytosol by an intramolecular interaction between the N-terminal regulatory region and the C-terminal catalytic domain, which is at least in part mediated by a 14-3-3 dimer bound to two phosphorylated residues (S259 and S621 in CRAF) (3). Upon activation, RAS binding to RAF results in RAF translocation to the plasma membrane where other activating steps take place. Key among these is the dephosphorylation of the inhibitory "S259" site (S259 in CRAF, S365 in BRAF, and S214 in ARAF), which leads to 14-3-3 dissociation, destabilizes the closed conformation of RAF, allows the cysteine-rich domain (CRD) to further anchor RAF to the membrane, and facilitates RAF dimerization (3).

A key phosphatase that mediates this dephosphorylation step is a heterotrimeric complex composed of MRAS, SHOC2, and protein phosphatase 1 (PP1) (4). SHOC2 is a ubiquitously expressed protein composed almost exclusively of leucine-rich repeats (LRRs) that was originally identified in *Caenorhabditis elegans* as a positive modulator of the ERK pathway (5, 6). A gain-of-function mutation in SHOC2 (S2G) is responsible for a subtype of Noonan syndrome (NS), a RASopathy characterized by short stature, congenital heart abnormalities, dysmorphic features, and intellectual disability (7). CRAF/RAF1 mutations are also frequently found in NS and cluster around the S259 14-3-3 binding site, enhancing CRAF activity through disruption of 14-3-3 binding (8) and highlighting the key role of this regulatory step in RAF–ERK pathway activation.

MRAS is a very close relative of the classical RAS oncoproteins (H-, N-, and KRAS, hereafter referred to collectively as "RAS") and shares most regulatory and effector interactions as well as transforming ability (9–11). However, MRAS also has specific functions of its own, and uniquely among RAS family GTPases, it can function as a phosphatase regulatory subunit when in complex with SHOC2 and PP1 to provide a key coordinate input required for efficient ERK pathway activation and transformation by RAS (4, 12). The mechanisms underlying this unique MRAS specificity remain to be elucidated. Activating mutations in MRAS are very rare in cancer but have recently been identified in NS (13). Mutations in *PPP1CB* have also been identified in NS, although they remain to be functionally characterized (14–16).

In this study, we have characterized biochemically the specificity of the SHOC2–MRAS–PP1 complex and identified key regions of SHOC2, MRAS, and PP1 required for complex formation. In addition to MRAS regions in the switch I, II, and

Significance

We demonstrate a mechanism whereby germline mutations in MRAS, SHOC2, and PPP1CB contribute directly to Noonan syndrome by enhancing formation of a ternary complex, which specifically dephosphorylates an inhibitory site on RAF kinases, activating downstream signaling. SHOC2 is required for tumorigenic properties of tumor-derived cell lines with RAS mutations and has more recently been identified by others in a synthetic lethal screen as a gene essential for viability of RAS mutant but not RAS wild-type cells. A thorough analysis of this complex at the biochemical and structural level has demonstrated the remarkable ability of this complex to dictate specificity for RAF and suggests possible strategies to inhibit the complex as a way of targeting the RAS–ERK pathway.

Author contributions: L.C.Y., N.H., and P.R.-V. designed research; L.C.Y., N.H., I.B.d.R., S.S., B.R.-T., J.R.W., and G.G.J. performed research; L.C.Y., F.M., and P.R.-V. analyzed data; and L.C.Y. and P.R.-V. wrote the paper.

Reviewers: D.K.M., National Cancer Institute–NIH; and M.T., University of Montreal.

The authors declare no conflict of interest.

[1]Present address: Helen Diller Family Comprehensive Cancer Center, University of California, San Francisco, CA 94158.

[2]Present address: Research Department of Structural and Molecular Biology, University College London, London WC1E 6BT, United Kingdom.

[3]To whom correspondence may be addressed. Email: frank.mccormick@ucsf.edu or p.rodriguez-viciana@ucl.ac.uk.

This article contains supporting information online at www.pnas.org/lookup/suppl/doi:10.1073/pnas.1720352115/-/DCSupplemental.

Published online October 22, 2018.

interswitch regions required for effector specificity, MRAS membrane localization is essential for complex activity towards RAF in vivo. Critically, we show that NS mutants of SHOC2, MRAS, and PP1β selectively promote complex formation and S259 RAF dephosphorylation, underscoring the critical role of this complex in regulation of the RAS–ERK pathway.

Results

The SHOC2–MRAS–PP1 Complex Functions as a Specific S259 RAF Phosphatase. We have previously shown that, when coexpressed in cells, active MRAS and SHOC2 form a complex with PP1 that efficiently dephosphorylates the S259 inhibitory site in RAF kinases (4, 12). To be able to further characterize the substrate specificity of the SHOC2–MRAS–PP1 complex in vitro, we developed a tandem affinity purification (TAP) strategy where high purity stoichiometric SHOC2–MRAS–PP1 complex could be purified after overexpression in HEK293 T-REx cells (*SI Appendix*, Fig. S1 *A–D*). This SHOC2–MRAS–PP1 complex efficiently dephosphorylates S259 CRAF and S365 BRAF but not other sites such as S338 CRAF/S445 BRAF or the inhibitory CRAF S43 and S289/S296/S301 sites (Fig. 1*A*). Thus, the SHOC2–MRAS–PP1 complex has specificity for the S259 inhibitory site even among RAF phosphorylation sites. Because of the better yield obtained in the purification of full-length BRAF compared with CRAF, BRAF protein was mostly used as a substrate in subsequent in vitro phosphatase experiments.

When comparing the SHOC2–MRAS–PP1 complex to other PP1 complexes that were purified using a similar TAP strategy, the SHOC2–MRAS–PP1 complex displays significantly increased ability to dephosphorylate S365 BRAF compared with other PP1 holocomplexes studied such as GADD34–PP1, SCRIB–PP1 (Fig. 1*B*), PNUTS–PP1 (Fig. 1*C*), SDS22–PP1 (Fig. 1*D*), or MYPT3–PP1 (*SI Appendix*, Fig. S1*G*). Because of their dimeric nature, we used an N-terminal EE-tagged PP1α for the TAP strategy of other PP1 holocomplexes. To rule out the possibility that this tag may negatively affect the activity of the PP1 holocomplexes in their comparison with SHOC2–MRAS–PP1 complex containing untagged PP1, a batch of SHOC2–MRAS–PP1 complex was generated using EE–PP1 in a strategy similar to that used for the other holocomplexes (Fig. 1*D*). After careful titration of PP1 levels, no significant differences were observed in the phosphatase activity of SHOC2–MRAS–PP1 complexes containing untagged or EE–PP1, ruling out any interference by the tag on PP1 (Fig. 1*D*). Taken together, the above results show that MRAS and SHOC2 function as substrate-specifying regulatory subunits for PP1, making the resulting holoenzyme a preferential S259 RAF phosphatase (Fig. 1*E*).

S365 BRAF dephosphorylation by the SHOC2–MRAS–PP1 complex in vitro is potently inhibited by the phosphatase inhibitor calyculin A (*SI Appendix*, Fig. S1 *E* and *F*) and at significantly higher concentrations by okadaic acid (*SI Appendix*, Fig. S1*H*). In contrast, a phosphatase inhibitor mixture containing the commonly used serine/threonine phosphatase inhibitors β-glycerophosphate and sodium pyrophosphate did not have any effect, nor did the tyrosine/alkaline phosphatase inhibitor sodium vanadate. Although PP1 is a metallophosphatase with two metal ions in its catalytic site, the metal chelator EDTA had no effect on SHOC2–MRAS–PP1 complex activity (*SI Appendix*, Fig. S1*G*). This pattern of inhibitor sensitivity inversely correlates with that of lambda phosphatase, which is potently inhibited by EDTA and sodium vanadate but not calyculin A or okadaic acid. We note that the insensitivity to EDTA of PP1 purified from mammalian sources is consistent with the presence of metals other than Mn^{2+} at the active site (Fe^{2+} and Zn^{2+}), which can also contribute to substrate specificity (17, 18).

SHOC2 Is Predicted to Structurally Resemble the A Subunit of PP2A and Uses Different Regions to Interact with MRAS/PP1 and SCRIB. Protein phosphatase 2A (PP2A) is a heterotrimeric holoenzyme that may serve as a framework for the SHOC2–MRAS–PP1 complex. The A subunit (PPP2R1A), which is composed of HEAT repeats, forms a horseshoe shape (Fig. 2*A*) that serves as a scaffold where the C subunit (PPP2AC) docks with the active site facing away from the scaffold (19). Binding of 1 of 18 known regulatory B subunits is thought to contribute to substrate specificity (20). SHOC2 is mostly composed of LRRs and has no sequence homology with PPP2R1A. However, as for other LRR-containing proteins (21), SHOC2 is predicted to form a horseshoe-shaped structure with striking similarity with PPP2R1A (Fig. 2 *A* and *B*).

To test whether either SHOC2 or PPP2R1A subunits have the potential to interact with components from the other complex,

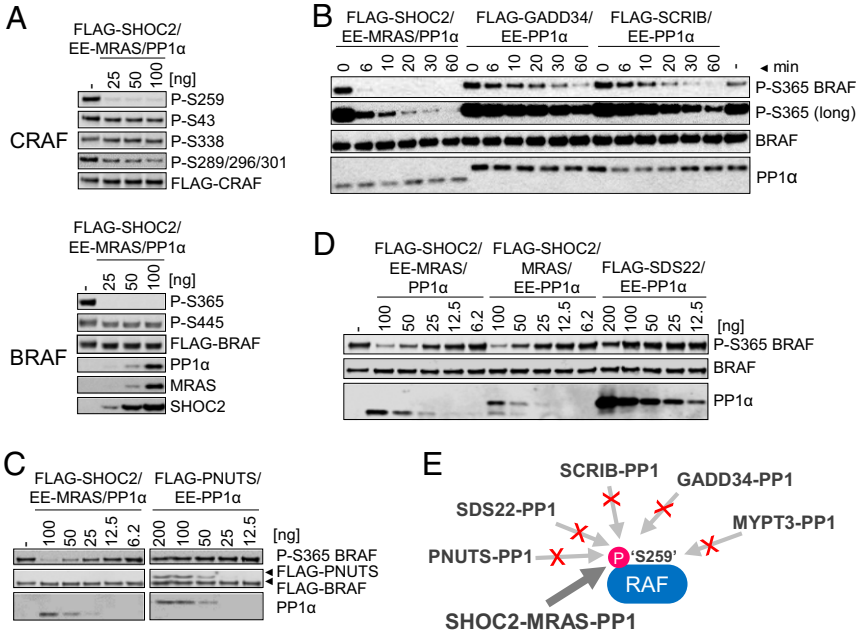

Fig. 1. The SHOC2–MRAS–PP1 complex functions as a RAF S259 phosphatase. (*A*) SHOC2–MRAS–PP1α complex has increased phosphatase activity in vitro against S259 CRAF/S365 BRAF compared to other phosphorylation sites. CRAF/BRAF were purified from cells pretreated with calyculin A to increase stoichiometry of phosphorylation of all possible phosphosites and incubated with SHOC2–MRAS–PP1α complex for 60 min at 37 °C. (*B*) SHOC2–MRAS–PP1α complex has increased phosphatase activity against S365 BRAF compared to GADD34–PP1α or SCRIB–PP1α complex. T6–BRAF was incubated with 10 nM PP1 complexes at 37 °C for the indicated times. (*C*) SHOC2–MRAS–PP1α complex has increased S365 BRAF phosphatase activity compared to PNUTS–PP1α. T6–BRAF was incubated with increasing amounts of PP1 complexes at 37 °C for 30 min. The band above T6–BRAF detected with the FLAG antibody corresponds to FLAG–PNUTS. (*D*) EE–N-terminal tag in PP1α does not affect phosphatase activity in vitro. SHOC2–MRAS–PP1 complexes containing PP1α with or without an EE tag were compared to each other and to SDS22–PP1α in a dose response as in *C*. (*E*) Summary of *B–D* highlighting substrate specificity of SHOC2–MRAS–PP1 complex against S365 BRAF compared to other PP1 holophosphatases.

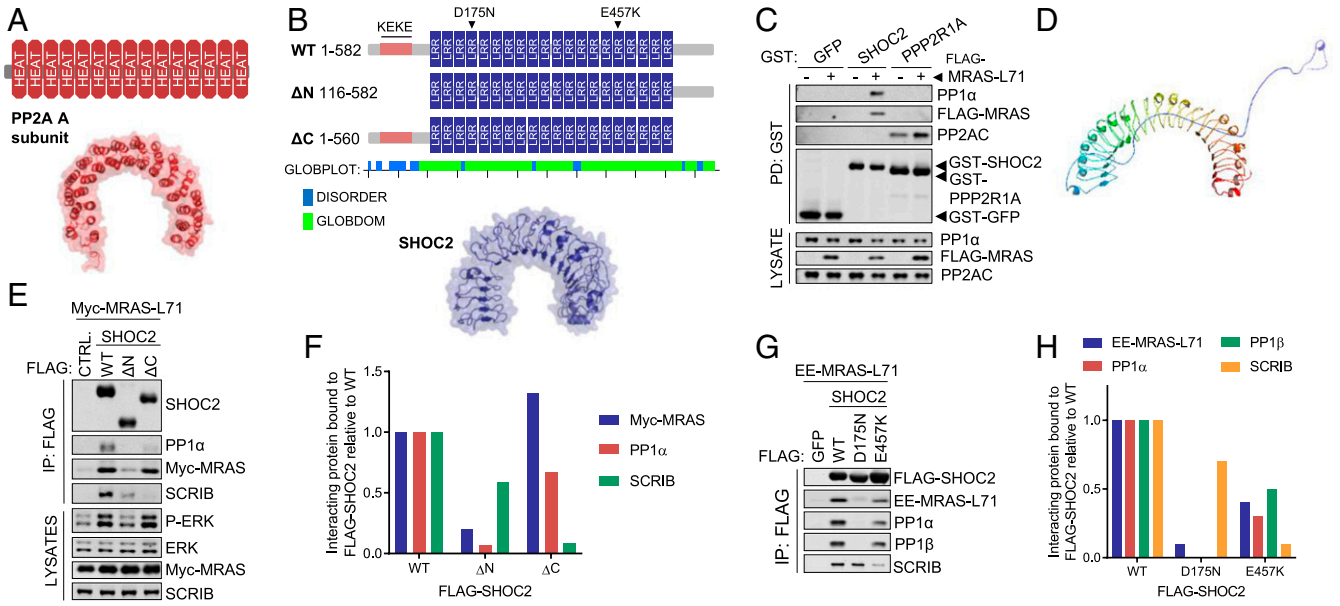

Fig. 2. SHOC2 is predicted to structurally resemble the A subunit of PP2A and uses different regions to interact with MRAS/PP1 and SCRIB. (*A*) Domain structure of the A subunit of PP2A (UNIPROT ID P30153) showing HEAT repeats and structure [Protein Data Bank (PDB) ID code 2IAE], visualized using PyMOL. (*B*) Domain structure of SHOC2 (UNIPROT ID Q9UQ13) showing mutants used, regions of disorder predicted by Globplot 2 (globplot.embl.de), and model generated with ITASSER using LRR domains (residues 102–560) (https://zhanglab.ccmb.med.umich.edu/I-TASSER). Tick marks on GLOBPLOT axis indicate 50-residues length. (*C*) SHOC2, but not the A subunit of PP2A (PPP2R1A), interacts with active MRAS and PP1, but not PP2A catalytic subunit (PP2AC). GST–SHOC2, –PPP2R1A, or –GFP (control) were cotransfected with empty vector or FLAG–MRAS–L71. GST pulldowns were probed with the indicated antibodies. (*D*) Domain structure of SHOC2 model of full-length SHOC2 structure generated by the Phyre2 server showing flexible/disordered N terminus (in blue) (www.sbg.bio.ic.ac.uk/phyre2). (*E*) SHOC2 N terminus is required for interaction with MRAS/PP1, whereas the C terminus interacts with SCRIB. FLAG–IPs and lysates of FLAG–SHOC2 WT or truncation mutants were probed as indicated. (*F*) Quantification of Myc–MRAS–L71, endogenous PP1, and SCRIB bound to FLAG–SHOC2 in *E* relative to WT SHOC2. (*G*) SHOC2 D175N and E457K differentially affect interaction with MRAS/PP1 and SCRIB. MRAS–L71 was cotransfected with FLAG–GFP (control), –SHOC2 WT, or mutants. (*H*) Quantification of proteins interacting with SHOC2 in *G*. Li-COR signal was divided by the FLAG–SHOC2 bait signal and plotted relative to SHOC2 WT.

GST–SHOC2 or –PPP2R1A were transfected into HEK293T cells. GST pulldowns show that, in the presence of active MRAS, SHOC2 interacts with PP1 and MRAS but not PP2AC, whereas PPP2R1A interacts with PP2AC but not PP1 or MRAS (Fig. 2*C*). Therefore, SHOC2 and PPP2R1A appear to have evolved independently as horseshoe-shaped scaffolds to form distinct heterotrimeric phosphatase complexes.

Like most PP1 regulators (22), SHOC2 has regions of intrinsic disorder (Fig. 2*B*). In particular, the N terminus of SHOC2 up to the first LRR, which contains a KEKE motif-rich region (23), is predicted to be unstructured (Fig. 2 *B* and *D*). To study a possible contribution to complex formation or activity, deletions of N- and C-terminal regions outside the LRR core were expressed in cells together with active MRAS. N-terminal deletion strongly disrupts complex formation with MRAS (consistent with ref. 24) and PP1 and is defective for ERK stimulation, but only has a modest effect on the interaction with SCRIB (Fig. 2 *E* and *F*). In contrast, deletion of the C-terminal residues of SHOC2 strongly disrupts the interaction with SCRIB, while only having a modest effect on the interaction with PP1 (Fig. 2 *E* and *F*).

Certain loss-of-function mutations identified in the *C. elegans* SHOC2 ortholog impair complex formation with PP1 and MRAS in the human SHOC2 protein (4). The D175N mutation, although defective for PP1 and MRAS binding, can still interact with SCRIB (Fig. 2 *G* and *H*). The E457K mutant is only partially impaired in complex formation with MRAS–PP1 but severely defective for interaction with SCRIB, consistent with SCRIB primarily interacting with the C-terminal region of SHOC2. Thus, multiple distinct regions of SHOC2 likely make independent contacts with MRAS–PP1 and SCRIB (*SI Appendix*, Fig. S2*B*).

SHOC2 Mutations in NS Enhances Complex Formation with MRAS and PP1. SHOC2 S2G mutations are responsible for a subtype of NS and behave as gain-of-function by creating a de novo myristoylation site that promotes SHOC2 association with the plasma membrane, and enhance ERK pathway activation in some contexts (7). An additional mutation in SHOC2, M173I, has been identified in an individual with a RASopathy phenotype, although surprisingly it was described as a loss-of-function mutant (25). To further shed light on the role of the SHOC2 as a RAF phosphatase in the context of NS, FLAG-tagged versions of both SHOC2 M173I and S2G were expressed together with active MRAS. Both SHOC2 Noonan mutants have increased ability to interact with MRAS and PP1 compared with WT SHOC2 (Fig. 3*A*). M173I and S2G SHOC2 also efficiently dephosphorylate S365 BRAF/S259 CRAF in cotransfection assays, although in the experimental conditions used overexpression of SHOC2 WT is very potent and stimulates near-complete RAF dephosphorylation, and no further increase can therefore be detected with NS mutants (Fig. 3 *B* and *C*). Regardless, these data show that M173I (and S2G) promote complex formation of a functional RAF phosphatase complex. Furthermore, when reexpressed in SHOC2 knockout DLD-1 cells, both S2G and M173I SHOC2 decrease the higher basal levels of S365 BRAF and S259 CRAF phosphorylation as well as the impaired EGF-induced ERK pathway activation caused by SHOC2 ablation (Fig. 3*D*). Serum-starved DLD-1 cells reexpressing SHOC2 S2G and M173I have modestly lower P-S365-BRAF and P-S259 CRAF levels and modestly higher P-MEK and P-RSK levels compared with WT SHOC2-expressing cells (Fig. 3*D*), which is consistent with RASopathy gain-of-function mutations being only weakly activating, and ERK pathway activation by such

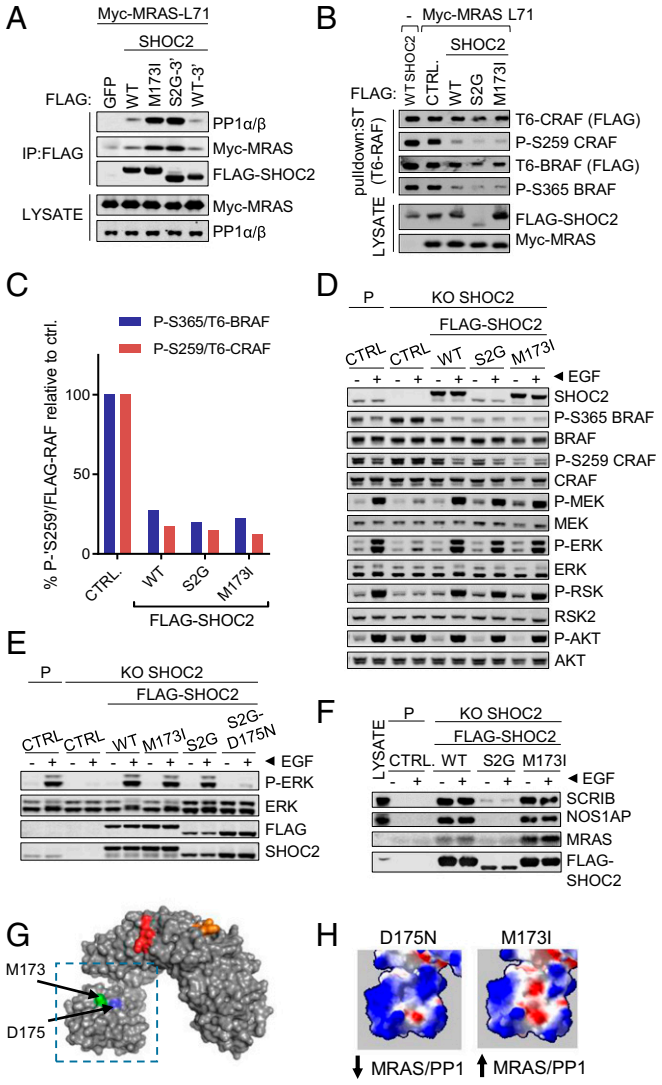

Fig. 3. SHOC2 mutations in NS enhances complex formation with MRAS and PP1. (*A*) FLAG IPs/lysates from HEK293T transfected with FLAG–SHOC2 WT/mutant or GFP plus Myc–MRAS–L71. SHOC2 S2G has a FLAG tag on the C terminus (labelled 3′), whereas for M173I the FLAG tag was provided by the vector and is at the N terminus (hence the molecular weight difference). SHOC2 WT with similar FLAG-tag configuration at either N- or C-term are shown at either side. (*B*) As in *A*, but in cells cotransfected with T6–BRAF and T6–CRAF. RAFs were pulled down with Strep-tactin (ST) beads and probed as indicated. (*C*) Quantification of BRAF and CRAF S365 dephosphorylation from *B*. (*D*) Lysates from DLD-1 SHOC2 knockout cells transduced with lentiviruses expressing either empty vector of FLAG–SHOC2 WT or mutants after serum starving and 5-min EGF treatment (25 ng/mL). (*E*) Lysates from cells as before including a SHOC2 double mutant (S2G/D175N) and stimulated with 5 ng/mL EGF for 5 min. (*F*) FLAG–SHOC2 IPs from cells used in *D*. (*G*) SHOC2 model of Fig. 1*B* (amino acids 102–560) with D175N (blue) and M173I (green) residues highlighted. SLVK (SILK-like) and KIPF (RVXF-like) motifs are highlighted in red and orange, respectively. (*H*) In silico modeling of D175N and M173I mutations with electrostatic potential computed using Swiss-PdbViewer. Positive charges are represented as blue, and negative charges as red. Region displayed is the boxed region of *E*, that is, the N terminus up to approximately residue L220.

mutants being difficult to detect in many experimental systems (*Discussion*) (7, 26). Inclusion of the D175N (loss-of-function) mutation in the S2G SHOC2 mutant prevented the rescue of the SHOC2 KO cells as measured by ERK activation levels in response to EGF stimulation (Fig. 3*E*). This suggests that the targeting of SHOC2–S2G to the membrane still requires interactions with MRAS and PP1 to exert its effects on the pathway.

When SHOC2 interactions in DLD-1 rescue cells were analyzed in FLAG–SHOC2 immunoprecipitates (IPs), the lower expression levels of SHOC2 S2G precluded detection of endogenous proteins. However, increased interaction with MRAS, but not with other SHOC2-interacting proteins such as SCRIB and NOS1AP (12), can be seen with SHOC2 M173I compared with WT (Fig. 3*F*). Taken together, our results suggest that both SHOC2 S2G and M173I RASopathy mutations function as a gain of function to up-regulate the ERK pathway during development by selectively promoting phosphatase complex formation with MRAS and PP1.

We note that genetics in *C. elegans* (D175N, loss-of-function) and RASopathies (M173I, gain-of-function; this study) have identified proximal residues in SHOC2 that can both negatively and positively modulate complex formation with MRAS–PP1 (Fig. 3 *G* and *H*). Furthermore, sequence alignment of the LRRs of SHOC2 and SDS22, another LRR protein that interacts with PP1, aligns SHOC2–D175 residue with SDS22–D148 (*SI Appendix*, Fig. S2*A*), a residue known to participate in interaction between SDS22 and PP1 (27). Taken together, these observations strongly suggest this area of SHOC2 will make contacts with MRAS and/or PP1 critical for complex formation (*SI Appendix*, Fig. S2*B*).

C-Terminal Residues of MRAS Are Not Required for SHOC2–PP1 Complex Formation or Phosphatase Activity in Vitro but Are Required for Efficient BRAF–S365 Dephosphorylation and ERK Pathway Activation in Vivo. Membrane targeting signals within their C-terminal hypervariable regions (HVR) localize RAS family GTPases to the plasma membrane. Excluding the CAAX motif, MRAS does not contain additional cysteines within its HVR that are targeted for palmitoylation in other RAS family members. Instead the HVR of MRAS contains multiple basic amino acids and thus resembles more closely the HVR of KRAS4B (Fig. 4*A*). Although the HVR is not required for RAS interaction with RAFs, plasma membrane localization is required for ERK pathway activation and transformation (28, 29). C-terminal mutants of MRAS (Fig. 4*A*) were used to examine whether the same was true for its effectors.

When coexpressed with SHOC2, substitutions of the C-terminal polybasic region (K5Q), deletion of the CAAX box (ΔCAAX) or of the last 30 residues comprising the HVR (MRAS 1–178 or ΔHVR) does not impair formation of the SHOC2–MRAS–PP1 complex (Fig. 4 *A* and *B*). In fact, deletion of the CAAX box or the HVR and the resulting cytosolic localization significantly enhances complex formation with MRAS–PP1 as well as AF6. In clear contrast, interaction with BRAF is impaired in ΔCAAX and ΔHVR mutants (Fig. 4*B*). Thus, membrane localization differentially contributes to MRAS interaction with different effectors.

Despite showing increased ternary complex formation with SHOC2–PP1, ΔCAAX and ΔHVR MRAS do not stimulate ERK phosphorylation (Fig. 4*B*), which correlates with their impaired ability to dephosphorylate BRAF S365 in cotransfection assays (Fig. 4*C*). To test the possibility that the MRAS HVR, although not required for SHOC2–MRAS–PP1 complex formation, could be required for its functional activity, the phosphatase activity of recombinant SHOC2–MRAS–PP1 complexes containing either WT or ΔHVR MRAS was compared in in vitro assays. WT and ΔHVR MRAS-containing SMP complexes had a very similar ability to dephosphorylate full-length BRAF in vitro (Fig. 4 *D* and *E*). Taken together, our data suggest that proximal localization at the membrane is required to bring the SHOC2–MRAS–PP1 complex into close proximity to its RAF substrate for efficient dephosphorylation and downstream pathway activation in vivo.

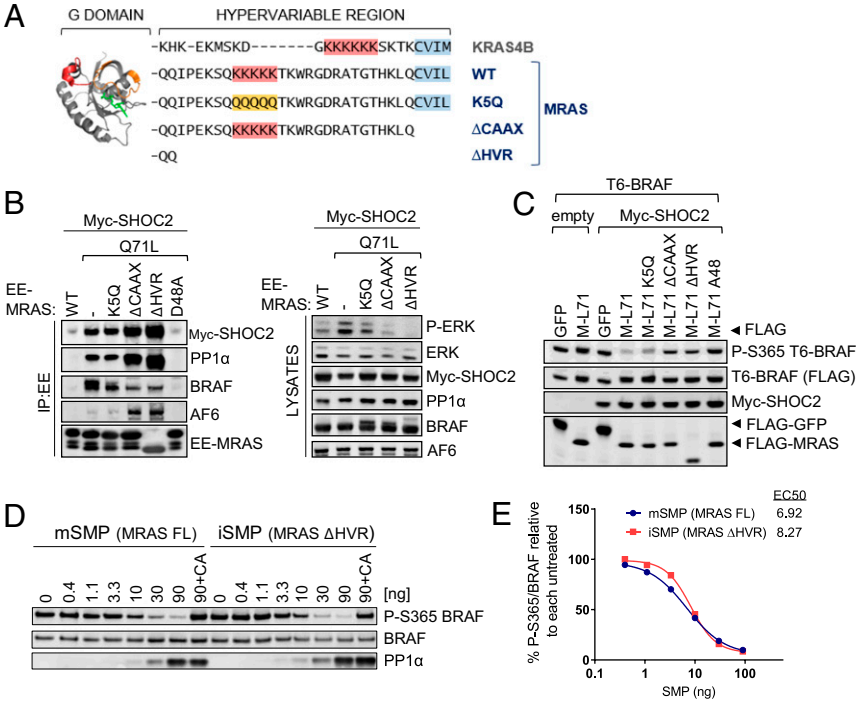

Fig. 4. C-terminal residues of MRAS are not required for SHOC2–PP1 complex formation or phosphatase activity in vitro but are required for efficient S365 BRAF dephosphorylation and ERK pathway activation in vivo. (*A*) Outline of MRAS C-terminal mutations used. Poly-lysine residues changed are shaded pink, and the CAAX box is shaded blue. (*B*) EE IPs and lysates of FLAG–EE–MRAS constructs were probed with the indicated antibodies. (*C*) The CAAX box and HVR are required for S365 BRAF dephosphorylation in vivo. Lysates from cells cotransfected with T6–BRAF and MRAS ("M") mutants were analyzed as in *B*. (*D*) The HVR is not required for S365 BRAF dephosphorylation in vitro. Different amounts of SHOC2–MRAS–PP1 complexes were incubated with T6–BRAF protein for 30 min at 37 °C. mSMP complex is purified from T-REx-293 mammalian cells and contains full-length MRAS, whereas iSMP is from Sf9 insect cells and contains MRAS ΔHVR. Where shown, calyculin A (CA) was added as control. (*E*) The SMP EC_{50} was derived from Li-COR quantification of *D*.

Residues in and Around the MRAS SWITCH I and Interswitch Regions Contribute to Its Effector Specificity. The three members of the RRAS subfamily (MRAS, RRAS, and TC21) contain an identical core effector domain as RAS proteins (32–40 in RAS) and share interactions with most effectors (11) (Fig. 5*A*). However, the ability to promote complex formation with SHOC2 and PP1 is uniquely specific to MRAS among many RAS family GTPases tested (12). To identify residues accounting for this striking effector specificity, a mutational study of MRAS was undertaken. Substitutions in the core effector domain of RAS have been shown to selectively disrupt interaction with different effectors such as RAF, RALGDS, and PI3K (e.g., ref. 30). However, the equivalent mutations in the MRAS effector domain disrupt binding to SHOC2–PP1 and B/CRAF binding similarly and thus do not discriminate between these effectors (Fig. 5*B*).

To identify residues in MRAS mediating SHOC2–PP1 specificity, residues in or adjacent to the switch I region were altered to match those of either RAS or RRAS (Fig. 5 *A*–*C*). Substitution of residues within switch I directly preceding the core effector domain to those found in RRAS (RRAS-like S36/Y37/S40 "SY-S") or mutation of residues between switch I and II domains (interswitch region) to that of RAS (RAS-like "QVV-GETCL") (Fig. 5*A*) strongly disrupt interaction with SHOC2–PP1 but have no effect on interaction with RAFs or AF6 (Fig. 5 *C*–*E*). The RAS-like L51R, immediately following switch I, increases binding to BRAF and CRAF while modestly impairing interaction with SHOC2–PP1. RAS-like LI–NH–DE (L33/I34/N36/H37/D40/E41) mildly impairs PP1 binding but increases interaction with AF6. In keeping with our model, reduction of SHOC2–PP1 binding to MRAS in the SY-S and QVV-GETCL mutants results in impaired ability of this MRAS mutants to stimulate BRAF dephosphorylation (Fig. 5*D*). Thus, multiple residues outside and within switch I are contributing to the specificity of MRAS effector binding (Fig. 5 *C*–*E*) with the interswitch region playing an important role not seen in other RAS-subfamily members (*Discussion*).

MRAS Mutations in Noonan Syndrome Have Enhanced SHOC2–MRAS–PP1 Complex Activity. G23V and T68I point mutations in MRAS were identified in patients with NS (13) (Fig. 6 *A* and *B*). Given that SHOC2 NS mutations stimulate complex formation (Fig. 3*E*), we addressed whether the same was true of MRAS mutations. Both MRAS mutants have increased SHOC2–PP1 binding compared with WT MRAS, which correlates with increased ability to activate the ERK pathway (Fig. 6*C*) and to dephosphorylate S365 BRAF in cotransfection assays (Fig. 6*D*).

MRAS G23V (equivalent to the oncogenic G13V in RAS), like MRAS Q71L (Q61L in RAS), also shows increased interaction with other effectors such as BRAF, CRAF, and AF6 (Fig. 6*C*), consistent with activating mutations leading to GTP-loading of MRAS (13). On the other hand, the T68I mutation, which is located in switch II, did not stimulate binding to BRAF or CRAF. This suggests that, while MRAS–G23V can drive RAF activation through both direct binding and complex formation with SHOC2–PP1, the MRAS–T68I substitution discriminates between effectors selecting specifically for interaction with SHOC2 and PP1 and thus the RAF phosphatase function of MRAS.

The Recurrent PP1β–P49R Mutation Identified in NS Selectively Enhances SHOC2–MRAS Binding. PP1 is known to interact with an extensive range of PP1-regulatory proteins through one or more of a number of docking motifs (such as RVxF, SILK, and MyPHONE) that bind to corresponding grooves on PP1 (31). Mutations in *PPP1CB*/PP1β have been described in patients with a RASopathy phenotype similar to NS with loose anagen hair (14–16) and in individuals with features overlapping NS (32, 33) (Fig. 7*A*). None of these mutations fall within the recognized catalytic or substrate-recognition regions of the phosphatase, suggesting they are more likely involved in interactions with regulatory proteins. Several of them, including the more common P49R, are located on the opposite side to the catalytic site around the SILK motif binding region. The equivalent residue in PP1γ has indeed been shown to interact with the SILK motif of the PP1-interacting protein inhibitor-2 (34) (Fig. 7*B*). Since we have previously shown that a degenerate SILK motif in SHOC2 (SLVK) is involved in PP1 binding (12), we chose to examine the effect of this recurrent mutation on interaction with SHOC2 as well as other known PP1-interacting proteins with SILK motifs such as SCRIB and SIPP1, as well as without such as MYPT1, which instead interacts with the

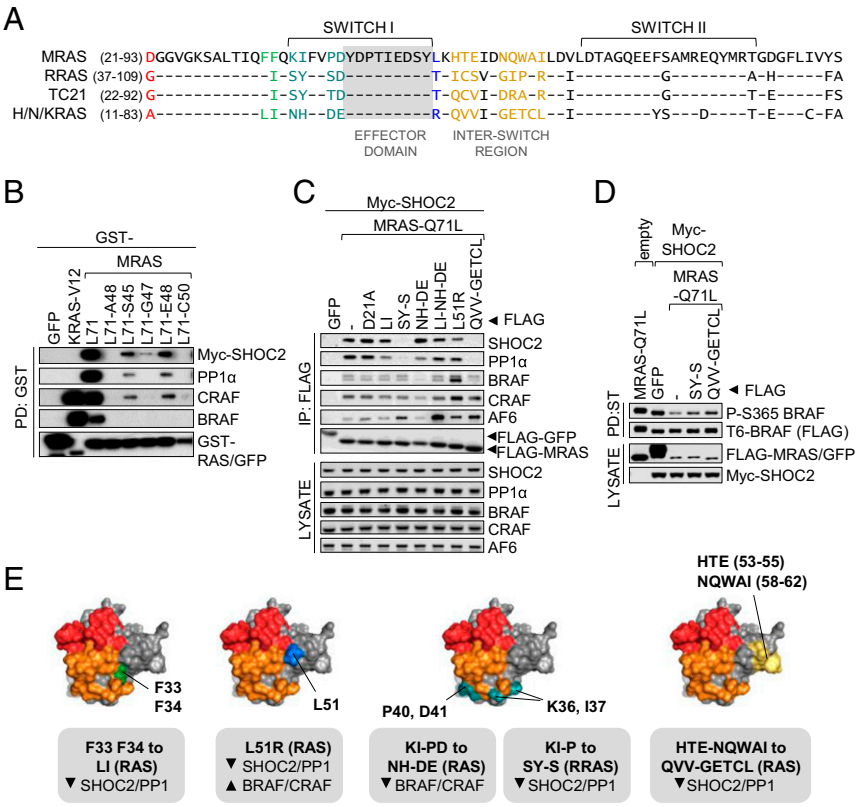

Fig. 5. Residues in and around the MRAS switch I and interswitch regions contribute to its effector specificity. (*A*) Alignment of selected MRAS residues with RRAS, TC21, and H/N/KRAS with selected residues studied highlighted. (*B*) GST–MRAS pulldowns from transfected HEK293 were probed with indicated antibodies and visualized with chemiluminescence. (*C*) FLAG–MRAS IPs were probed for the indicated antibodies and visualized with Li-COR Odyssey (except AF6, which was chemiluminescence). (*D*) Strep-tactin pulldowns of T6–BRAF were assessed for P-S365 phosphorylation in the presence of SHOC2 and MRAS–Q71L mutants. (*E*) Structure of MRAS (PDB ID code 1X1R) with Switch I (orange) and Switch II (red) with residues highlighted that, when mutated to those of RRAS or RAS, alter effector binding (also indicated underneath).

RvXF and MyPHONE binding grooves of PP1 (PP1β but not PP1α) (35, 36).

In cells cotransfected with active myc-MRAS, IPs of FLAG–PP1β show that the P49R mutation increases the interaction with MRAS and endogenous SHOC2 compared with WT. On the other hand, interaction with SIPP1 is impaired, whereas binding to SCRIB or MYPT1 is unaffected (Fig. 7*E*). Similar results are observed with the equivalent P50R substitution on the highly conserved PP1α isoform (Fig. 7*E*). To further explore the contribution of the SILK as well as RVxF binding grooves to the interaction with SHOC2, we generated substitutions in amino acids in PP1 regions known to interact with the SILK and RVxF motifs of other interacting proteins (34, 36) (Fig. 7 *B–D*).

In the absence of coexpressed MRAS, endogenous SHOC2 can be readily detected in complex with PP1β P49R, whereas interaction with WT PP1β is at the limit of sensitivity for detection in our experimental conditions (Fig. 7*F*). However, coexpression of MRAS Q71L greatly stimulates SHOC2 binding to WT PP1β, and in this context substitutions in both SILK (E53A/L54A and E115A/F118A) and RVxF (D241A/L242A, C290R, L288R) binding pockets potently disrupts SHOC2 interaction with FLAG–PP1β (Fig. 7*F*). In contrast, interaction with MYPT1 (which contains an RVxF motif but lacks a SILK motif) is unaffected by MRAS expression and is disrupted by substitutions in the RVxF but not SILK-binding pockets (Fig. 7*F*).

Taken together, these observation strongly suggest that both the RVxF and SILK binding grooves in PP1 provide points of contact for SHOC2 and show that the recurrent PP1β P49R RASopathy mutation, located within the SILK binding groove, is selectively gain-of-function for interaction with SHOC2–MRAS, but none of the other PP1 interactors tested (*Discussion*).

Discussion

SHOC2, originally identified as a positive modulator of the RAS–ERK pathway in *C. elegans* (5, 6), functions together with MRAS–GTP and PP1 in a phosphatase complex that specifically dephosphorylates the conserved S259 inhibitory site in RAF kinases. Striking substrate specificity can be observed in vitro with

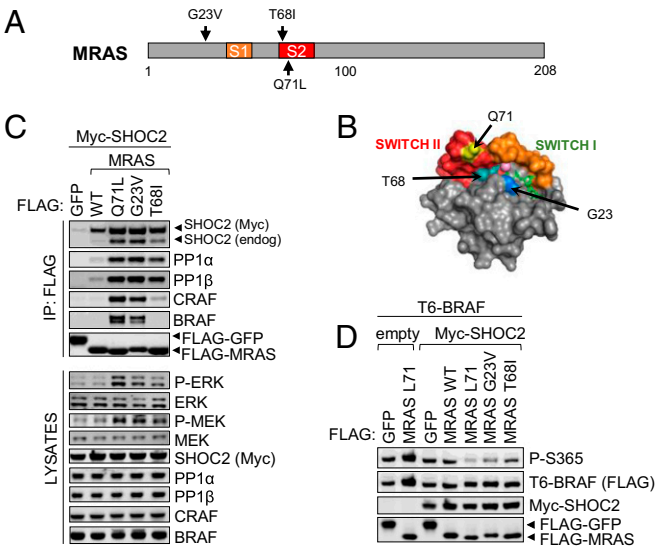

Fig. 6. MRAS mutations in NS have enhanced SHOC2–MRAS–PP1 complex activity. (*A*) Positions of NS mutations (*Upper*) and the activating Q71L mutation within MRAS. (*B*) Model of MRAS (PDB ID code 1X1R) showing locations of residues in *A*: G23 (blue), T68 (turquoise), Q71 (yellow); Switch I (orange), Switch II (red), GDP (green sticks), and Mg^{2+} (pink sphere). (*C*) FLAG IPs/lysates from cells transfected with Myc–SHOC2 and either GFP (control) or MRAS WT/mutants were probed with indicated antibodies. (*D*) P-S365 levels on transfected T6–BRAF were assessed in response to combinations of transfected empty vector/Myc–SHOC2 and GFP/MRAS WT/mutants.

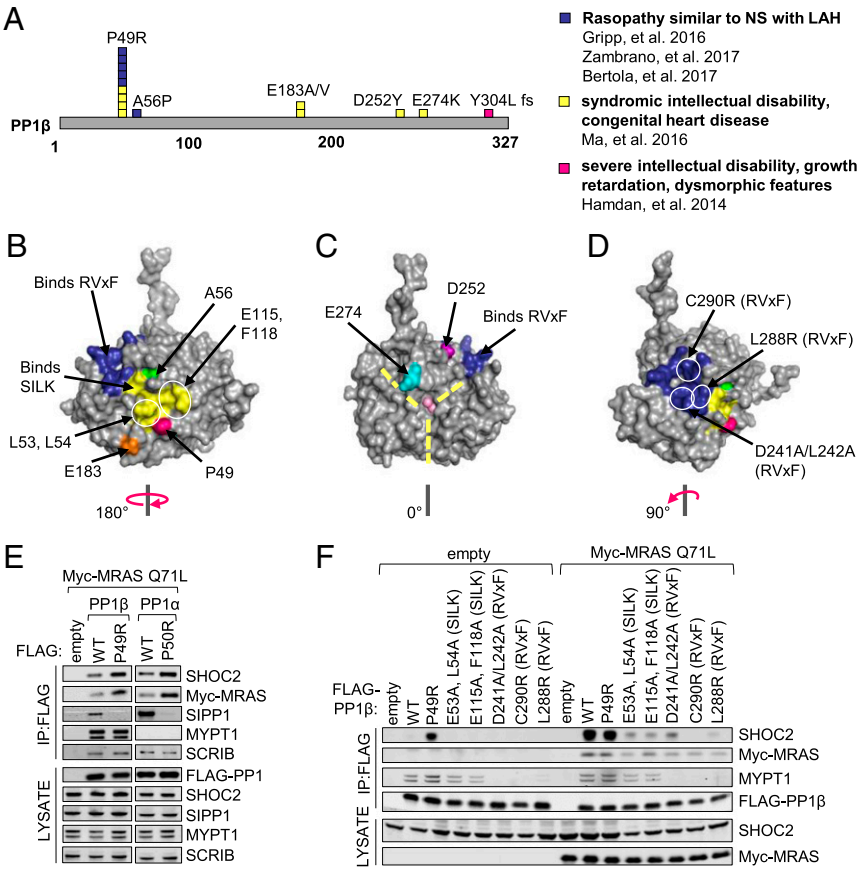

Fig. 7. The recurrent PP1β–P49R mutation identified in NS selectively enhances SHOC2–MRAS binding. (*A*) Positions of syndromic mutations in PP1β. (*B*) Positions of mutations in *A* in the 3D structure of PP1β (from PDB ID code 1S70) (rear side of structure in *C*). SILK and RVxF binding grooves highlighted in yellow and purple, respectively. Mutated SILK-binding residues used in *F* are circled. Y301I (not indicated) is the result of a base insertion and causes a frameshift of the terminal amino acids. (*C*) As in *B*, but showing the side of PP1β on which the catalytic site is located, with Mg^{2+} (pink sphere) and substrate binding grooves (dashed lines) shown. (*D*) Rotation of structure in *C* to show locations of indicated mutated residues within the RVxF-binding region (*F*). (*E*) FLAG IPs and lysates from cells transfected with WT/mutant PP1α and PP1β and active MRAS. (*F*) As in *E*, comparing SILK- and RVxF-binding mutants of PP1.

recombinant SHOC2–MRAS–PP1 complex against S365 BRAF/S259 CRAF but not other RAF phosphorylation sites and compared with PP1 complexes with other regulatory proteins (Fig. 1). The structure of the PP2A holoenzyme illustrates well how regulatory proteins could dictate phosphatase specificity by creating a different physiochemical landscape of the active site compared with the individual catalytic subunit, as well as different surface areas for substrate recruitment (20). The in vitro enzymatic data in this study are consistent with such a scenario, and we speculate that MRAS–GTP and SHOC2 change the physiochemical landscape around the active site of PP1 to provide specificity for S259 RAF dephosphorylation.

We have previously shown that S259 dephosphorylation is more readily detected on the RAF that coimmunoprecipitates with RAS than on the total RAF population (4), consistent with the SHOC2–MRAS–PP1 complex preferentially dephosphorylating the pool of RAF recruited by RAS to the plasma membrane. Membrane localization of RAS is not required for its interaction with RAF but is required for RAF and ERK pathway activation (28, 29). Similarly, membrane localization of MRAS is not required for complex formation with SHOC2 and PP1 but is required for RAF dephosphorylation and ERK pathway activation (Fig. 4). MRAS is regulated by the same GEFs and GAPs that regulate RAS activation (37), and it is therefore expected that upon activation by extracellular signals, MRAS–GTP will promote complex formation with SHOC2–PP1 at the same plasma membrane microdomains where RAS is concomitantly activated. Proximal positioning in 2D is predicted to increase binding constant by five orders of magnitude relative to free solution (38). Proximal positioning of the SHOC2–MRAS–PP1 complex at the membrane is thus expected to greatly promote dephosphorylation of the S259 inhibitory site on the RAS-bound RAF. MRAS thus also behaves as a substrate-targeting subunit within the complex.

Although SHOC2 has no sequence homology with the A subunit of PP2A, as for other LRR proteins it is predicted to form a horseshoe-shaped structure with remarkable similarities to the PP2A A subunit. SHOC2 and PP2A A subunit may provide a case of convergent structural evolution, where different protein sequences have evolved to form a similarly shaped scaffold to support a phosphatase heterotrimeric holoenzyme by bringing together a catalytic subunit (PP1 or PP2AC) with an additional regulatory subunit (MRAS or B subunit, respectively). In the case of PP2A, the conformation of the A subunit changes from a twisted hook shape in monomeric form to a tight horseshoe shape when in complex with B and C subunits (20). Equivalent conformational rearrangements are likely to apply to SHOC2. Many proteins, including some that regulate PP1, contain intrinsically disordered regions that become structured in the presence of a binding partner (22, 39). Degenerate RvXF and SILK motifs in SHOC2 lie at either side of a region of predicted disorder in LRR 11 (12). Further modeling of SHOC2 predicts a flexible hinge role for LRR 13 (23), further supporting a dynamic role for this region in complex formation. The N terminus of SHOC2, which contains the nuclear export KEKE motifs (23), is also predicted to be disordered and is required for complex formation with PP1 and MRAS as well (Fig. 2). We speculate that, upon initial binding to MRAS–GTP, these disordered regions in SHOC2 may become structured within the ternary complex allowing for multiple points of contact and a synergistic interaction with PP1 and MRAS (*SI Appendix*, Fig. S2 *B* and *C*).

Genetics point to an additional region of SHOC2 involved in complex formation. D175N was identified as a loss-of-function mutation in the *C. elegans* SHOC2 ortholog (5, 6) and disrupts interaction with PP1 and MRAS but not SCRIB (Fig. 2).

A substitution in an adjacent SHOC2 residue, M173I, was found in an individual with a RASopathy phenotype (25). Although reported as a loss of function, we find that M173I behaves as a gain-of-function mutant that has enhanced interaction with MRAS and PP1 and rescues ERK activation in SHOC2-deficient cells. The SHOC2 S2G mutation more frequently found in NS creates a de novo myristoylation site that promotes membrane association (7) and also increases interaction with MRAS and PP1 (Fig. 3) likely by proximal positioning to MRAS at the membrane, increasing the binding constant.

The ability to interact with SHOC2 and PP1 appears to be uniquely specific to MRAS among over 30 RAS family GTPases tested (12). We show that at least some of this striking specificity comes from residues within the switch I region that are unique to MRAS (Fig. 5). We have also identified the region between switch I and II domains (interswitch region) as being required for MRAS interaction with SHOC2–PP1 but not other MRAS effectors. Although the interswitch region has not been previously implicated in effector binding in RAS GTPases, it is structurally sensitive to the GDP/GTP cycle and involved in effector interactions in ARF and RAB GTPases (40–42).

MRAS mutations in NS also shed light on effector specificity. In contrast to G23V, which increases interactions with all MRAS effectors tested, T68I, which resides in the switch II region, selectively stimulates interaction with SHOC2 and PP1 but not other effectors such as RAF. Thus, although MRAS G23V can contribute to ERK pathway up-regulation by both direct interaction with RAFs and SHOC2–PP1, T68I appears to drive NS by specific gain-of-function complex formation with SHOC2–PP1. Selection for specific effectors has already been encountered in a RASopathy setting: In Costello syndrome, HRAS–G60D (also in switch II) enhances interaction with RAF but not with PIK3CA, RALGDS, or PLCE1 (26). T68I MRAS also appears to be a weaker activating mutation than G23V. This is consistent with previous observations on the equivalent T58I mutation in HRAS and KRAS in RASopathies. HRAS T58I in Costello syndrome displays a more attenuated phenotype than the more frequent G12 mutations (43). KRAS T58I is found in NS, whereas other mutations such as P34R give rise to the more severe phenotype of cardiofaciocutaneous syndrome (44).

With regards to regions of PP1 involved in complex formation with SHOC2–MRAS, several lines of evidence suggest the both RvXF and SILK binding pockets are likely to provide points of contact for SHOC2 binding. Several of the RASopathy PP1β mutations lie around or within this SILK binding region, and the position equivalent to the recurrent PP1β P49R in PP1γ (P50) is part of a pocket that interacts with the leucine in the Inhibitor-2 SILK motif (GILK) (34). We now show that P49R PP1β increases affinity for SHOC2–MRAS. Future studies should determine whether other PP1β RASopathy mutations also modulate interaction with SHOC2–MRAS and thus identify additional points of contact. Interestingly, PP1β P49R differentially modulates interaction with PP1 interactors, even among those binding to the SILK region: It increases interaction with SHOC2–MRAS, has no effect on SCRIB binding, and decreases SIPP1 binding. A selective gain-of-function interaction is also seen with MRAS T68I, which increases affinity for SHOC2–PP1 but not other MRAS effectors, and with SHOC2 M173I, which increases interaction with MRAS–PP1 but not other SHOC2-interacting proteins such as SCRIB. Therefore, in the context of RASopathies, mutations in SHOC2–PP1–MRAS complex members select for increased interaction with the other complex members but not necessarily other interactors and thus for the S259 RAF phosphatase function of the subunits (but not necessarily other functions).

Patients with PP1β P49R mutation have RASopathies that most closely resemble NS with loose anagen hair caused by SHOC2 S2G, which conversely promotes interaction with PP1–MRAS (14–16). This strongly suggests P49R PP1β up-regulates the RAS–ERK pathway to drive a RASopathy primarily through increased activity of the SHOC2–MRAS–PP1 complex. However, a contribution from impaired SIPP1 binding to the pathogenic features of PP1β P49R cannot be ruled out, particularly in light of the pathogenesis of mutations of the SIPP1-interacting protein polyglutamine-binding-tract binding protein-1 (PQBP1). PQBP1 is mutated in syndromes with X-linked mental retardation (45) that, in addition to intellectual disability, also feature short stature and congenital heart defects, which overlap phenotypes observed in NS patients. SIPP1 has been suggested to target PP1 to dephosphorylate splicing factors (46), and impairment of SIPP1 binding to PP1β–P49R may therefore alter splicing and contribute to the pathogenic features of this syndromic mutant. Furthermore, in addition to disrupting SIPP1 binding, P49R could also modulate, positively or negatively, interaction with other PP1 interactors not tested in this study, particularly those containing SILK motifs.

It is widely accepted that strong activation of the RAS–ERK pathway is not tolerated during development, and RASopathy gain-of-function mutations have to be mild enough as to not be embryonic lethal. Experimentally detecting increased RAS–ERK pathway activation by such weakly activating RASopathy mutations has thus often proven difficult (e.g., refs. 7 and 26). Consistently, it is often difficult to reproducibly show increased ERK phosphorylation by SHOC2, PP1β, and MRAS T68I NS mutants in the experimental systems used in this study. It has been proposed that rather than hyperactivating ERK activity, as in an oncogenic scenario, these mutations may contribute to elevated or sustained pathway activity in response to particular growth factors and/or cell types (7, 26). Regardless, ours as well as other studies (26) suggest that measuring protein interactions in cells provides a more sensitive assay to assess mild gain-of-function RASopathy mutations.

In summary, we show in this study that NS mutations in SHOC2, MRAS, and PP1β selectively increase ternary complex formation of a phosphatase holoenzyme that specifically dephosphorylates "S259" RAF, a site that functions as an inhibitory 14-3-3 binding site. Gain-of-function mutations in RAF1 are also frequently found in NS and cluster around the S259 site to disrupt 14-3-3 binding (8, 47). Thus, the genetics of NS underscore the key role of the SHOC2–MRAS–PP1 complex in S259 RAF dephosphorylation and RAF–ERK pathway dynamics.

We have previously proposed that the SHOC2–MRAS–P1 complex has properties of an attractive therapeutic target for ERK pathway inhibition in RAS-driven tumors (4, 12). SHOC2 was recently identified as one of five genes necessary for proliferation of RAS mutant but not RAS–wild-type acute myeloid leukemia cell lines (48) and in a screen to overcome BRAF inhibitor resistance in BRAF mutant cells (49, 50), further strengthening the case for the SHOC2 complex as a therapeutic target. Phosphatase inhibitors continue to lag well behind kinase inhibitors in drug discovery, but there is increasing evidence that serine/threonine phosphatase holoenzymes represent underexplored targets of pharmacological inhibition. Pending resolution of its crystal structure, this study suggests possible strategies to inhibit the SHOC2–MRAS–PP1 complex. Allosteric inhibition is an emerging theme in phosphatases (51–54), and there is now proof of concept of specific inhibition of a PP1 holophosphatase by small molecules binding to its regulatory subunit (55). Inhibition of substrate binding, as is the case with the immunosuppressants FK506 and cyclosporin inhibition of PP2B/calcineurin (56), is also an attractive possibility. Targeting PP1 directly away from the catalytic pocket may also be a viable strategy. It has been proposed that targeting the small surface grooves in PP1 involved in interaction with particular PP1-interaction motifs (such as the SILK motif) would only inhibit selected PP1 holoenzyme subsets (31). The syndromic PP1β P49R provides proof of concept for such an approach as it shows that substitutions around the SILK binding groove can differentially modulate interaction even among the

reduced number of SILK-containing PP1 interactors. The 173–175 region of SHOC2 may also provide an attractive candidate region for small molecules to disrupt the SHOC2–MRAS–PP1 complex as substitutions in this region can both positively and negatively regulate complex formation (Fig. 3). The crystal structure of the SHOC2–MRAS–PP1 complex should greatly assist in driving a drug discovery effort to target this unique RAS–ERK pathway component.

Materials and Methods

Purification of Recombinant Proteins. SHOC2–MRAS–PP1α complex was purified from T-REx-293 (Thermo Fisher Scientific) "T-8" cells using a tandem affinity strategy, as outlined in *SI Appendix*, Fig. S1*A*. Other PP1 holoenzymes (GADD34/PP1α, MYPT3/PP1α, SDS22/PP1α, and SHOC2/MRAS/PP1α used in Fig. 1*D*) were transiently coexpressed as FLAG–PP1Rs and EE–PP1α in HEK293 cells. FLAG–mSCRIB/EE–PP1α was generated after transient transfection into 2T-shSHOC2 cells (with stable SHOC2 knockdown). Cells were washed with PBS and lysed in PBS-M lysis buffer [PBS, pH 7.4, 1% (wt/vol) Triton X-100, 5 mM $MgCl_2$, 0.1 mM $MnCl_2$, 1 mM DTT, and protease inhibitor mixture (Roche)] and phosphatase inhibitor solution (10 mM NaF, 2 mM Na_3VO_4, 2 mM $Na_4P_2O_7$, and 2 mM β-glycerophosphate). Extracts were centrifuged at 20,000 × *g* for 20 min at 4 °C and incubated with FLAG beads (Millipore Sigma) for 2–4 h at 4 °C while rotating. Beads were washed with TBS–MMX (20 mM Tris, pH 7.5, 150 mM NaCl, 5 mM $MgCl_2$, 0.1 mM $MnCl_2$, 0.1% Triton X-100, and 5 mM β-mercaptoethanol) and eluted with 100 μg/mL FLAG peptide (F4799; Millipore Sigma). Eluate was added onto EE-antibody–linked agarose beads, incubated for 2 h at 4 °C while rotating, washed with TBS–MMX, and eluted with 100 μg/mL GluGlu peptide (3× CEEEEYMPME).

T6 (TAP6) BRAF protein was purified from HEK293T cells stably expressing pLEX–TAP6–BRAF. The TAP6 tag is tandem array of tags containing SBP, 2× HIS, 3× Strep, and FLAG tags followed by a TEV protease cleavage site. Cells were lysed (with lysis buffer as above except 1 mM EDTA and no $MgCl_2$) and cleared as above, and incubated with Strep-tactin (Millipore Sigma) beads rotating for 2 h at 4 °C. Beads were washed five times with PBS/0.1% Triton X-100/500 mM NaCl/5 mM β-mercaptoethanol, and then equilibrated in 20 mM Tris, pH 7.5/0.1% Triton X-100/100 mM NaCl/5 mM β-mercaptoethanol. BRAF was eluted in the same buffer containing 2.5 mM desthiobiotin, which was subsequently removed through dialysis. FLAG–BRAF/CRAF were purified similarly to T6–BRAF except using transiently transfected HEK293T cells, FLAG beads, and elution with FLAG peptide as for PP1 complexes above. In addition, cells were treated with 100 nM calyculin A 20 min before lysis to increase phosphorylation of RAF.

In Vitro Phosphatase Assays. In vitro phosphatase assays were performed in PP1 buffer (20 mM Hepes, pH 7.5, 100 mM NaCl, 5 mM $MgCl_2$, 0.1 mM $MnCl_2$, 5 mM β-mercaptoethanol, and 0.1 mg/mL BSA) using 200 ng of BRAF as substrate. BRAF substrate was diluted in PP1 buffer and pretreated with inhibitors on ice for 15 min where applicable, followed by incubation at 30 or 37 °C with PP1 complexes. Reactions were stopped by adding NuPAGE sample buffer (Thermo Fisher Scientific), and dephosphorylation of BRAF was visualized by Western blotting with P-S365 BRAF and total BRAF or FLAG antibodies. Phosphatase inhibitor mixture (IC) used is as described in *Purification of Recombinant Proteins*.

Plasmids and Transient Transfection. Constructs were generated by cloning cDNA into the pENTR vector, and expression plasmids were generated using the Gateway system (Invitrogen). Site-directed mutagenesis was carried out on pENTR plasmids according to ref. 57. Transient transfection was performed by incubating plasmid and polyethylenimine (PEI) (Polysciences) in OptiMEM (Thermo Fisher Scientific) (at a ratio of 4 μg of PEI to 1 μg of plasmid) for 20 min before addition to cells. Fresh medium was added 16 h after transfection, and cells were lysed on the following day.

Cell Culture and Generation of Stable Cell Lines. HEK293 and DLD-1 cells were cultured in DMEM supplemented with 10% FBS at 37 °C under 5% CO_2. For EGF stimulation, cells were serum-starved in DMEM/0.5% FBS for at least 6 h followed by treatment with 25 ng/mL EGF, unless stated otherwise.

Lentiviruses were generated by transient transfection of HEK293 cells with the lentiviral construct, pMD.G and p8.91 packaging vectors. Virus-containing medium was harvested 48 and 72 h after transfection and supplemented with 5 μg/mL Polybrene (hexadimethrine bromide; Millipore Sigma). Cells were transduced with lentivirus, and where required, selection was carried out with either 2.5 μg/mL puromycin, 200 μg/mL hygromycin, or 1 mg/mL G418. T-REx-293 cells were cultured in 5 μg/mL blasticidin to maintain expression of the Tet repressor.

For generation of T-8 cell lines described in *SI Appendix*, Fig. S1, T-REx-293 cells were subjected to three sequential rounds of lentiviral infection with pLEX–MCS (Dharmacon) SHOC2–FLAG, pLenti–CMV/TO–Neo (Addgene; plasmid 17292) expressing EE–MRAS–Q71L, and pLenti–CMV/TO–Hygro (Addgene; plasmid 17291) expressing untagged PPP1CA. Dox-inducible constructs were a gift from Eric Campeau, currently affiliated with Zenith Epigenetics Corp, Alberta, Canada (58).

HEK293 cells expressing shRNA to SHOC2 have been previously characterized (12). Briefly, cells were transduced with lentivirus as above generated from pGIPZ–shSHOC2 (5′–3′ CTGCTGAAATTGGTGAATT) (Thermo Fisher Scientific), were selected with puromycin, and knockdown was assessed by Western blot.

DLD-1 SHOC2 KO cells were generated by transient transfection with the pSpCas9(BB)–2A–GFP (PX458), which was a gift from Feng Zhang, Broad Institute, Cambridge, MA (Addgene; plasmid 48138), containing a GFP expression cassette and the following gRNA-encoding sequence targeting exon 3 of SHOC2: 5′-gRNA-3′ GAGCTACATCCAGCGTAATG, PAM: AGG. GFP-positive cells were sorted by FACS into 96-well plates, and single-cell clones were analyzed by Western blot to assess SHOC2 protein levels. DLD-1 SHOC2 KO cells were then transduced with lentivirus expressing an empty vector, FLAG–SHOC2 WT, or different FLAG–SHOC2 mutants: D175N, E457K, M173I, SILK–KIPF, and 3′-FLAG S2G. After being selected with puromycin, reexpression of WT or mutant SHOC2 was assessed by Western blot.

Cell Lysis and Interaction Assays. Cells were lysed in PBS with 1% Triton X-100, protease inhibitor mixture (Roche), phosphatase inhibitor solution as before, and 1 mM EDTA (except where GTPase interactions were concerned and EDTA was substituted for 5 mM $MgCl_2$). Tagged proteins were immunoprecipitated/pulled down from cleared lysates using either FLAG (M2) agarose (Millipore Sigma), glutathione Sepharose beads (GE Healthcare), or EE (Glu–Glu) beads, and rotation at 4 °C for 2 h. Resins were washed with PBS/1% Triton X-100/1 mM EDTA or 5 mM $MgCl_2$ buffer and after draining were resuspended in NuPAGE LDS sample buffer (Thermo Fisher Scientific) before SDS/PAGE and Western blotting. Antibodies to the FLAG tag were from Millipore Sigma. Antibodies to PP1α, GST, SCRIB, BRAF, P-S43 CRAF, CRAF, MYPT1, RSK, P-S380 RSK, NOS1AP, and AF6 were from Santa Cruz Biotechnology. Antibodies to Myc, P-T202/Y204 ERK, ERK, P-S473 AKT, AKT, P-S217/221 MEK, MEK, P-S259 CRAF, P-286/296/301 CRAF, P-S338 CRAF, and P-S445 BRAF were from Cell Signaling Technology. Antibodies to PP1β, SIPP1/WPBP11, and EE tag were from Bethyl Laboratories, and the PP2AC antibody was from BD Transduction Laboratories. SHOC2 and MRAS and antibodies were generated as previously described (4, 12); P-S365 BRAF antibody was generated in-house against the QRDRSS{pSer}APNVHIC peptide. HRP- and DyLight-conjugated secondary antibodies for Western blotting were from GE Healthcare and Thermo Fisher Scientific, respectively. Membranes were visualized on either an Odyssey scanner (Li-COR) or Image Quant system (GE Healthcare).

ACKNOWLEDGMENTS. We thank Dhirendra Simanshu for critical reading of this manuscript.

1. Sebolt-Leopold JS, Herrera R (2004) Targeting the mitogen-activated protein kinase cascade to treat cancer. *Nat Rev Cancer* 4:937–947.
2. Rauen KA (2013) The RASopathies. *Annu Rev Genomics Hum Genet* 14:355–369.
3. Lavoie H, Therrien M (2015) Regulation of RAF protein kinases in ERK signalling. *Nat Rev Mol Cell Biol* 16:281–298.
4. Rodriguez-Viciana P, Oses-Prieto J, Burlingame A, Fried M, McCormick F (2006) A phosphatase holoenzyme comprised of Shoc2/Sur8 and the catalytic subunit of PP1 functions as an M-Ras effector to modulate Raf activity. *Mol Cell* 22:217–230.
5. Selfors LM, Schutzman JL, Borland CZ, Stern MJ (1998) soc-2 encodes a leucine-rich repeat protein implicated in fibroblast growth factor receptor signaling. *Proc Natl Acad Sci USA* 95:6903–6908.
6. Sieburth DS, Sun Q, Han M (1998) SUR-8, a conserved Ras-binding protein with leucine-rich repeats, positively regulates Ras-mediated signaling in *C. elegans*. *Cell* 94:119–130.
7. Cordeddu V, et al. (2009) Mutation of SHOC2 promotes aberrant protein N-myristoylation and causes Noonan-like syndrome with loose anagen hair. *Nat Genet* 41:1022–1026.
8. Molzan M, et al. (2010) Impaired binding of 14-3-3 to C-RAF in Noonan syndrome suggests new approaches in diseases with increased Ras signaling. *Mol Cell Biol* 30:4698–4711.
9. Chan AM, Miki T, Meyers KA, Aaronson SA (1994) A human oncogene of the RAS superfamily unmasked by expression cDNA cloning. *Proc Natl Acad Sci USA* 91:7558–7562.

10. Kimmelman A, Tolkacheva T, Lorenzi MV, Osada M, Chan AM (1997) Identification and characterization of R-ras3: A novel member of the RAS gene family with a non-ubiquitous pattern of tissue distribution. *Oncogene* 15:2675–2685.
11. Rodriguez-Viciana P, Sabatier C, McCormick F (2004) Signaling specificity by Ras family GTPases is determined by the full spectrum of effectors they regulate. *Mol Cell Biol* 24:4943–4954.
12. Young LC, et al. (2013) An MRAS, SHOC2, and SCRIB complex coordinates ERK pathway activation with polarity and tumorigenic growth. *Mol Cell* 52:679–692.
13. Higgins EM, et al. (2017) Elucidation of *MRAS*-mediated Noonan syndrome with cardiac hypertrophy. *JCI Insight* 2:e91225.
14. Bertola D, et al. (2017) The recurrent PPP1CB mutation p.Pro49Arg in an additional Noonan-like syndrome individual: Broadening the clinical phenotype. *Am J Med Genet A* 173:824–828.
15. Gripp KW, et al. (2016) A novel rasopathy caused by recurrent de novo missense mutations in PPP1CB closely resembles Noonan syndrome with loose anagen hair. *Am J Med Genet A* 170:2237–2247.
16. Zambrano RM, et al. (2017) Further evidence that variants in PPP1CB cause a rasopathy similar to Noonan syndrome with loose anagen hair. *Am J Med Genet A* 173: 565–567.
17. Chu Y, Lee EY, Schlender KK (1996) Activation of protein phosphatase 1. Formation of a metalloenzyme. *J Biol Chem* 271:2574–2577.
18. Heroes E, et al. (2015) Metals in the active site of native protein phosphatase-1. *J Inorg Biochem* 149:1–5.
19. Groves MR, Hanlon N, Turowski P, Hemmings BA, Barford D (1999) The structure of the protein phosphatase 2A PR65/A subunit reveals the conformation of its 15 tandemly repeated HEAT motifs. *Cell* 96:99–110.
20. Cho US, Xu W (2007) Crystal structure of a protein phosphatase 2A heterotrimeric holoenzyme. *Nature* 445:53–57.
21. Kobe B, Kajava AV (2001) The leucine-rich repeat as a protein recognition motif. *Curr Opin Struct Biol* 11:725–732.
22. Peti W, Nairn AC, Page R (2013) Structural basis for protein phosphatase 1 regulation and specificity. *FEBS J* 280:596–611.
23. Motta M, et al. (2016) SHOC2 subcellular shuttling requires the KEKE motif-rich region and N-terminal leucine-rich repeat domain and impacts on ERK signalling. *Hum Mol Genet* 25:3824–3835.
24. Jeoung M, Abdelmoti L, Jang ER, Vander Kooi CW, Galperin E (2013) Functional integration of the conserved domains of Shoc2 scaffold. *PLoS One* 8:e66067.
25. Hannig V, Jeoung M, Jang ER, Phillips JA, 3rd, Galperin E (2014) A novel SHOC2 variant in rasopathy. *Hum Mutat* 35:1290–1294.
26. Gripp KW, et al. (2015) An attenuated phenotype of Costello syndrome in three unrelated individuals with a HRAS c.179G>A (p.Gly60Asp) mutation correlates with uncommon functional consequences. *Am J Med Genet A* 167A:2085–2097.
27. Ceulemans H, et al. (2002) Binding of the concave surface of the Sds22 superhelix to the alpha 4/alpha 5/alpha 6-triangle of protein phosphatase-1. *J Biol Chem* 277: 47331–47337.
28. Warne PH, Viciana PR, Downward J (1993) Direct interaction of Ras and the amino-terminal region of Raf-1 in vitro. *Nature* 364:352–355.
29. Zhang XF, et al. (1993) Normal and oncogenic p21ras proteins bind to the amino-terminal regulatory domain of c-Raf-1. *Nature* 364:308–313.
30. Rodriguez-Viciana P, et al. (1997) Role of phosphoinositide 3-OH kinase in cell transformation and control of the actin cytoskeleton by Ras. *Cell* 89:457–467.
31. Bollen M, Peti W, Ragusa MJ, Beullens M (2010) The extended PP1 toolkit: Designed to create specificity. *Trends Biochem Sci* 35:450–458.
32. Ma L, et al. (2016) De novo missense variants in PPP1CB are associated with intellectual disability and congenital heart disease. *Hum Genet* 135:1399–1409.
33. Hamdan FF, et al. (2014) De novo mutations in moderate or severe intellectual disability. *PLoS Genet* 10:e1004772.
34. Hurley TD, et al. (2007) Structural basis for regulation of protein phosphatase 1 by inhibitor-2. *J Biol Chem* 282:28874–28883.
35. Scotto-Lavino E, Garcia-Diaz M, Du G, Frohman MA (2010) Basis for the isoform-specific interaction of myosin phosphatase subunits protein phosphatase 1c beta and myosin phosphatase targeting subunit 1. *J Biol Chem* 285:6419–6424.
36. Terrak M, Kerff F, Langsetmo K, Tao T, Dominguez R (2004) Structural basis of protein phosphatase 1 regulation. *Nature* 429:780–784.
37. Ohba Y, et al. (2000) Regulatory proteins of R-Ras, TC21/R-Ras2, and M-Ras/R-Ras3. *J Biol Chem* 275:20020–20026.
38. Simanshu DK, Nissley DV, McCormick F (2017) RAS proteins and their regulators in human disease. *Cell* 170:17–33.
39. Tompa P (2012) Intrinsically disordered proteins: A 10-year recap. *Trends Biochem Sci* 37:509–516.
40. Khan AR, Ménétrey J (2013) Structural biology of Arf and Rab GTPases' effector recruitment and specificity. *Structure* 21:1284–1297.
41. Pasqualato S, Renault L, Cherfils J (2002) Arf, Arl, Arp and Sar proteins: A family of GTP-binding proteins with a structural device for "front-back" communication. *EMBO Rep* 3:1035–1041.
42. Mishra A, Eathiraj S, Corvera S, Lambright DG (2010) Structural basis for Rab GTPase recognition and endosome tethering by the C2H2 zinc finger of early endosomal autoantigen 1 (EEA1). *Proc Natl Acad Sci USA* 107:10866–10871.
43. Gripp KW, Lin AE (2012) Costello syndrome: A Ras/mitogen activated protein kinase pathway syndrome (rasopathy) resulting from HRAS germline mutations. *Genet Med* 14:285–292.
44. Schubbert S, et al. (2006) Germline KRAS mutations cause Noonan syndrome. *Nat Genet* 38:331–336.
45. Kalscheuer VM, et al. (2003) Mutations in the polyglutamine binding protein 1 gene cause X-linked mental retardation. *Nat Genet* 35:313–315.
46. Llorian M, et al. (2005) Nucleocytoplasmic shuttling of the splicing factor SIPP1. *J Biol Chem* 280:38862–38869.
47. Pandit B, et al. (2007) Gain-of-function RAF1 mutations cause Noonan and LEOPARD syndromes with hypertrophic cardiomyopathy. *Nat Genet* 39:1007–1012.
48. Wang T, et al. (2017) Gene essentiality profiling reveals gene networks and synthetic lethal interactions with oncogenic Ras. *Cell* 168:890–903.e15.
49. Whittaker SR, et al. (2015) Combined Pan-RAF and MEK inhibition overcomes multiple resistance mechanisms to selective RAF inhibitors. *Mol Cancer Ther* 14: 2700–2711.
50. Kaplan FM, et al. (2012) SHOC2 and CRAF mediate ERK1/2 reactivation in mutant NRAS-mediated resistance to RAF inhibitor. *J Biol Chem* 287:41797–41807.
51. Chen YN, et al. (2016) Allosteric inhibition of SHP2 phosphatase inhibits cancers driven by receptor tyrosine kinases. *Nature* 535:148–152.
52. De Munter S, Köhn M, Bollen M (2013) Challenges and opportunities in the development of protein phosphatase-directed therapeutics. *ACS Chem Biol* 8:36–45.
53. Gilmartin AG, et al. (2014) Allosteric Wip1 phosphatase inhibition through flap-subdomain interaction. *Nat Chem Biol* 10:181–187.
54. Krishnan N, et al. (2014) Targeting the disordered C terminus of PTP1B with an allosteric inhibitor. *Nat Chem Biol* 10:558–566.
55. Carrara M, Sigurdardottir A, Bertolotti A (2017) Decoding the selectivity of eIF2α holophosphatases and PPP1R15A inhibitors. *Nat Struct Mol Biol* 24:708–716.
56. Peti W, Page R (2015) Strategies to make protein serine/threonine (PP1, calcineurin) and tyrosine phosphatases (PTP1B) druggable: Achieving specificity by targeting substrate and regulatory protein interaction sites. *Bioorg Med Chem* 23:2781–2785.
57. Laible M, Boonrod K (2009) Homemade site directed mutagenesis of whole plasmids. *J Vis Exp* 2009:1135.
58. Campeau E, et al. (2009) A versatile viral system for expression and depletion of proteins in mammalian cells. *PLoS One* 4:e6529.